



A new method for monitoring far-field noise level with a few near-field sensors

Xiaobin Cheng¹, Xun Wang, Jun Yang, Jing Tian

Key Laboratory of Noise and Vibration, Institute of Acoustics, Chinese Academy of Science, Beijing, China

ABSTRACT

The noise of electrical equipment operating outdoors in the residential areas, such as the transformers, is a growing concern. The sound of the equipment propagating to people's home should be monitored. It is sometimes convenient to measure the acceleration on the equipment or the sound pressure nearby but inconvenient to measure the sound pressure at the position of interest. This paper presents a new method to estimate the noise of the equipment with the sensors close to the equipment instead of the on-site sensors in the far field. This method employs the ideas of frequency response function measurement, and it first measures the response-response matrix from the neighbouring sensors to microphones at the desired location under different operational conditions. Then the sound pressure level under the new operational conditions can be calculated through the historical response-response matrices. The condition number of the matrix can be used to evaluate the errors and as a criterion to optimize the sensors' positions. The measurement results of a steel cylinder is also shown.

Keywords: Sound pressure monitoring I-INCE Classification of Subjects Number(s): 72.1

1. INTRODUCTION

The noise of electrical equipment, such as the transformers, propagating to people's home should be monitored. When the equipment is produced or newly repaired, the noise propagating to the residential area should also be known. The direct way to measure the sound pressure is to place the microphone at the location of interest. Sometimes, however, it is not convenient to place the microphone at the desired location. Regarding the noise monitoring of the electrical transformers, it is not convenient to always place the microphone at the remote position near people's home but is acceptable to place the sensors, which could be the accelerometers or microphones, close to the transformers. For instance, the accelerometers could be mounted on the transformer and the microphone are positioned only half meter away from the transformer. Therefore the sound pressure level(SPL) at the remote positions near people's home has to be estimated through these neighbouring sensors.

The relationship between the sensors at the neighboring positions and the microphones at the remote positions can be described by the methodology of the Transfer Function Analysis(TPA). The TPA method is implemented in the automotive industry to predict the SPL at the driver's ear using the accelerometers on the engine mount, gearbox or suspensions under operational conditions.(1, 2, 3). The similar problems, named as virtual sensor, are encountered in the active noise control technique (4, 5). Since the microphones cannot be placed at the position of people's ear, the SPL at people's ear should be estimated by remote microphones.

This paper demonstrates a new method which predicts the sound pressure of the transformer's noise at the target location by the accelerometers on the casing. The formula derivation, the experimental results and error analysis are shown.

2. METHOD

2.1 Response-response matrix

Regarding the sound propagating from the source to the receiver's position, the acoustic signal at the receiver's position is the convolution of the source signal with the impulse response of this acoustic system. Represented in the frequency domain, the signal of the receiver is the multiplication of the excitation signal by the transfer function. If two sources present simultaneously, the transfer function matrix \mathbf{H} from the sources to two reference receivers can be written as Eq. 1

¹xb_cheng@mail.ioa.ac.cn

$$\mathbf{X} = \mathbf{HS}$$

$$\begin{bmatrix} x_1(\omega) \\ x_2(\omega) \end{bmatrix} = \begin{bmatrix} h_{11}(\omega) & h_{12}(\omega) \\ h_{21}(\omega) & h_{22}(\omega) \end{bmatrix} \begin{bmatrix} s_1(\omega) \\ s_2(\omega) \end{bmatrix} \quad (1)$$

where $\begin{bmatrix} x_1(\omega) \\ x_2(\omega) \end{bmatrix}$ represents the signal captured by the receivers and $\begin{bmatrix} s_1(\omega) \\ s_2(\omega) \end{bmatrix}$ represents the sources signal at the excitation points.

Considering a third sensor, the transfer function \mathbf{T} from the sources to the third sensor is described as Eq. 2.

$$\mathbf{Y} = \mathbf{TS}$$

$$y_1(\omega) = \begin{bmatrix} T_{11}(\omega) & T_{12}(\omega) \end{bmatrix} \begin{bmatrix} s_1(\omega) \\ s_2(\omega) \end{bmatrix} \quad (2)$$

where $y_1(\omega)$ is the signal obtained by the third sensor. Since only two sources are considered here, the signal of the third sensor can be expressed by combing Eq. 1 with Eq. 2. The resulting relationship between signal of two reference response points and the third response point is Eq. 3

$$\mathbf{Y} = \mathbf{AX} \quad (3)$$

where

$$\mathbf{A} = \mathbf{TH}^{-1} \quad (4)$$

Despite no priori information about the transfer function matrices \mathbf{T} and \mathbf{H} , as long as the system is linear and time-invariant, the response-response matrix \mathbf{A} can be calculated by the operational data.

Assuming that the magnitude and phase of the sources vary under different operational conditions like Eq. 5, where n means the n -th operational condition, the response-response matrix \mathbf{A} can be obtained by calculating the Moore-Penrose Pseudoinverse of the operational data (Eq. 6).

$$\begin{bmatrix} y_{11}(\omega) & y_{12}(\omega) & \cdots & y_{1n}(\omega) \\ y_{21}(\omega) & y_{22}(\omega) & \cdots & y_{2n}(\omega) \end{bmatrix} = \begin{bmatrix} a_{11}(\omega) & a_{12}(\omega) \\ a_{21}(\omega) & a_{22}(\omega) \end{bmatrix} \begin{bmatrix} x_{11}(\omega) & x_{12}(\omega) & \cdots & x_{1n}(\omega) \\ x_{21}(\omega) & x_{22}(\omega) & \cdots & x_{2n}(\omega) \end{bmatrix}$$

$$\mathbf{Y} = \mathbf{AX} \quad (5)$$

$$\mathbf{A} = \mathbf{YX}^+ \quad (6)$$

where "+" represents the Moore-Penrose Pseudoinverse.

Under the new operational condition, the sound pressure \mathbf{Y}_{new} at the remote position can be obtained by multiplying by the aforementioned response-response matrix \mathbf{A} with the newly measured data \mathbf{X}_{new} (Eq. 7). In this way, the sound pressure at a remote location could be monitored by the reference accelerometers on the equipment casing. It is not necessary to always place the microphones at the remote location.

$$\mathbf{Y}_{\text{new}} = \mathbf{AX}_{\text{new}} \quad (7)$$

The reference sensors could be more than the sources, in that case, the overdetermined Pseudoinverse should be implemented. The number of sources may not be limited by two, this method is still applicable as long as the number of reference sensors is no less than the number of sources.

2.2 Condition number

The key point of this response-response matrix based sound pressure estimation method is to calculate the Moore-Penrose Pseudoinverse of the operational data. The sensitivity to the measurement errors with respect to the matrix inversion can be described by the condition number. The measurement errors resulting from the low signal-to-noise ratio could be amplified due to the large condition number (6). In order to overcome this kind of ill-conditioned problem, Singular Value Decomposition(SVD) (7) and matrix regulation (8) are developed to calculate the inverse ill-conditioned matrix accurately.

The operational data \mathbf{X} is the multiplication of the excitation signal by the transfer function matrix, and the condition number for multiplying two matrices is larger than the condition number of each matrix individually as illustrated in Eq. 8 (6).

$$\kappa(\mathbf{X}) \geq \kappa(\mathbf{H}), \kappa(\mathbf{S}) \quad (8)$$

where κ represents the condition number. If sources' conditions does not change considerably, the condition number with regard to \mathbf{X} could be large. Meanwhile, if the two reference sensors are too close to each other or the transfer functions from the two sources to the two reference sensors are identical at certain particular frequencies. The transfer function matrix \mathbf{H} are ill-posed, the overall operational data matrix \mathbf{X} are ill-conditioned as well.

Since the vibration modal of the equipment is very complicated, it could happen that at certain frequencies the operational matrix \mathbf{X} is ill-conditioned, while at another frequency the operational matrix is well-conditioned. The robust way to guarantee the estimation accuracy is using additional reference sensors to provide low condition number for the whole frequency range of interest.

3. EXPERIMENTAL RESULTS

3.1 Experimental set-up

Tests were carried out on a steel cylinder with a flat plate inserted inside as illustrated in Fig. 1. Referring to the figure, one shaker is mounted on the upper side of the inner wall, and the other on the plate. Linear sweep signals are generated simultaneously by using both shakers in the frequency range between 1000Hz and 1100Hz under three operational conditions. The magnitude of excitation signals from the upper shaker under Condition 1 is reduced by -10dB under Condition 2 and -14dB under Condition 3 respectively, meanwhile the magnitude from the lower shaker remains constant throughout the three conditions.

One microphone is located three meters away from the cylinder for measurement of the SPL in the far-field. In contrast, signals captured by five accelerometers are used to validate the new method for the prediction of the SPL. As illustrated in Fig. 1, two accelerometers at positions P1 and P2 are directly attached to the shakers and the other three on the outer casing located at positions P3-P5. Accelerometer-measured signals under Conditions 1 and 2 are used to determine the response-response matrix in order to predict the SPL under Condition 3, as addressed in Section. 2.1

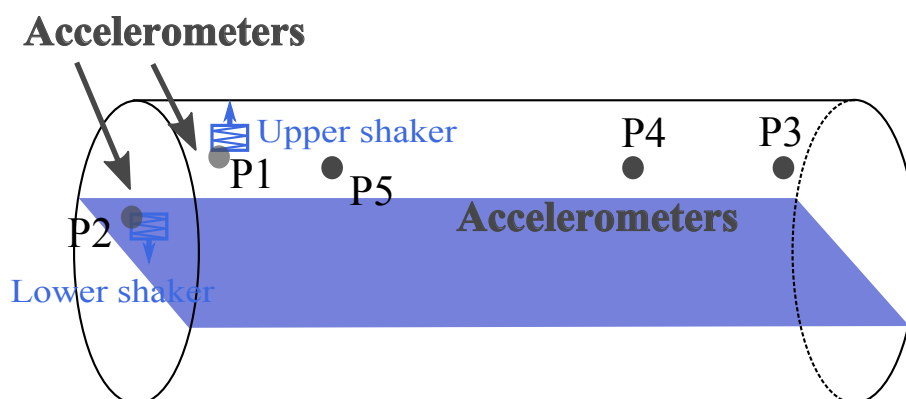


Figure 1 – Arrangement of shakers and sensors. Three accelerometers are mounted on the outer casing and two accelerometers are attached on two shakers respectively.

3.2 SPL measurements

To evaluate the effects of condition number on the accuracy of the SPL prediction, accelerometer-measured data at P1 and P2 are selected in the calculation comparing to those chosen from P3-P5. For data measured

at P1 and P2 where the two accelerometers are directly attached to the shakers, the transfer function matrix \mathbf{H} is almost diagonal indicating it is well-conditioned. In this case, it can be seen from Fig. 2 that there is a good agreement between the measured and predicted SPL. Fig. 2 also gives the corresponding condition number in the excitation frequency. For accelerometer-measured data at P3 and P4, it is shown in Fig. 3 that the predicted SPL generally matches the measured result except at around 1054Hz and 1061Hz, where the condition numbers are considerably large in particular at 1061Hz.

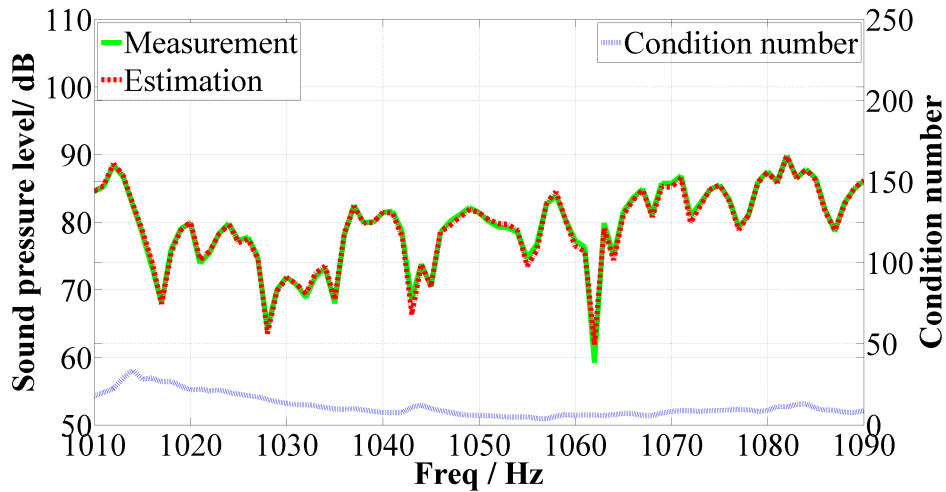


Figure 2 – Comparison of the measured and estimated SPL using the accelerometers-measured data at P1 and P2. The condition number at the corresponding frequencies is referred.

Additional check of the transfer function matrix reveals that the discrepancy at 1061Hz is caused by the vibration node. Fig. 4 plots each element of the transfer function matrix from the upper and lower shakers to the chosen accelerometers at P3 and P4. The transfer functions from the upper and lower shakers to P3 are relatively small at 1061 Hz comparing to the transfer function from the upper shaker to P4. Throughout the measurements, the magnitude of excitation signals only from the upper shaker is changed, the excitation signal from the lower shaker is kept unchanged. As a consequence, the column vectors of the operational data \mathbf{X} is not changed significantly. This leads to a high condition number and hence large prediction errors at certain frequencies due to the vibration node.

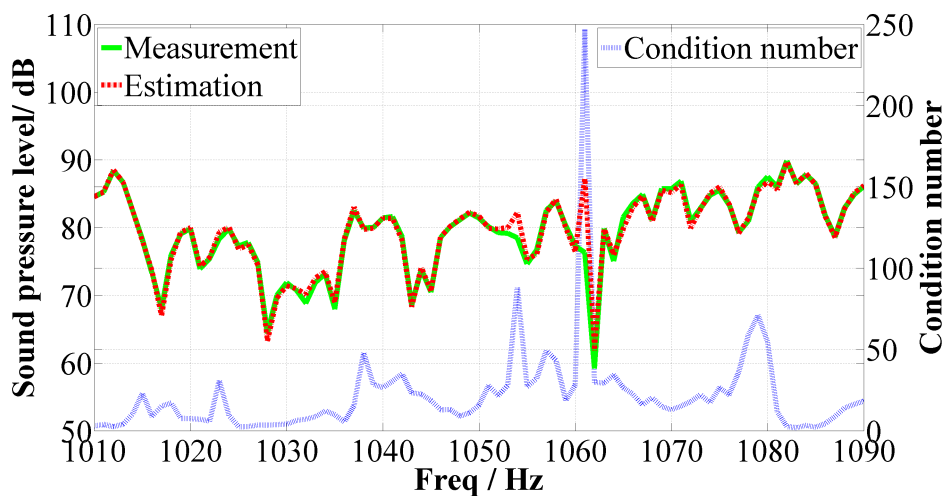


Figure 3 – Comparison of the measured and estimated SPL using the accelerometers-measured data at P1 and P2. The condition number at the corresponding frequencies is referred.

Fig. 5 plots the predicted SPL using selected accelerometer-measured data at P3-P5 in comparison with the measured SPL. When two accelerometer-measured data are chosen, it can be seen from the figure that the best agreement with the measured SPL is achieved by using data captured at P4 and P5. Good agreements between the measured and predicted SPL can be achieved over the entire frequency range except at around 1054Hz and 1061Hz using P3 and P4, and around 1022Hz, 1043Hz and 1068Hz using P3 and P5. Only slight improvement can be made using all the data captured at P3-P5. This suggests that if the reference sensors are correctly selected, there is no need to using additional sensors.

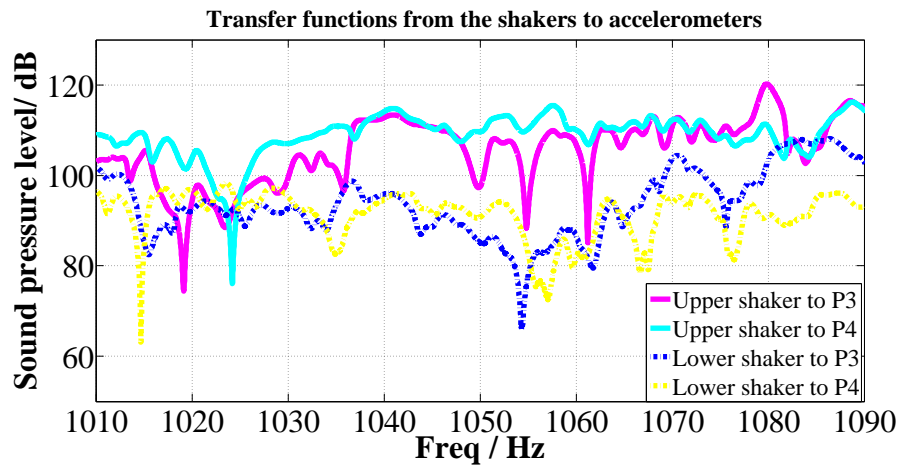


Figure 4 – Transfer functions from the shakers to the chosen accelerometers at P3 and P4

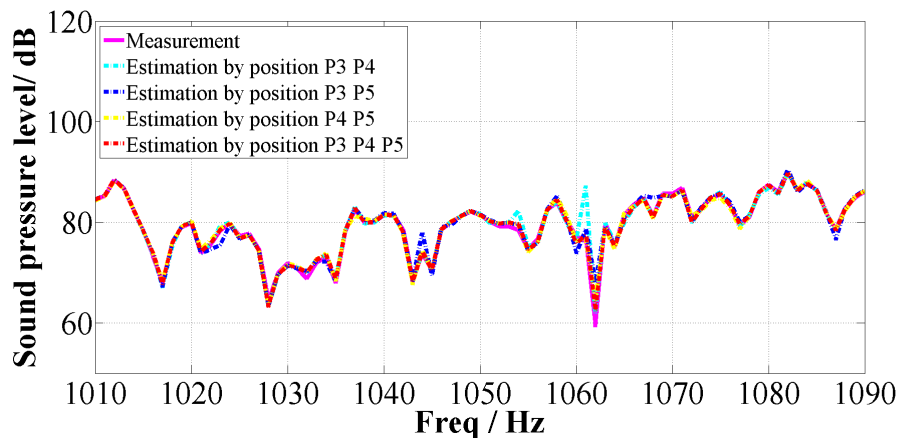


Figure 5 – Comparison of measured and predicted SPL using selected accelerometer-measured data at P3-P5

4. DISCUSSION AND FURTHER WORK

This paper presents a novel approach to predict the SPL in the far field by using the near-field sensors. The fundamental theory has been provided and the criterion for evaluation of the effectiveness of the prediction is made based on the condition number. Experiments were carried out to validate the effectiveness of the new method for the SPL prediction. It has been found that the accuracy of the prediction can be largely improved by adopting the correct sensor positions. Vibration nodes of the equipment will be taken into account for optimal design of sensor positions. More SPL measurements are being undertaken on the test rig to corroborate the theoretical predictions.

REFERENCES

1. Ákos Gajdáty P. Advanced Transfer Path Analysis Methods. Katholieke Universiteit Leuven; 2011.

2. Martin Lohrmann TH. Operational Transfer Path Analysis: Comparison with Conventional Methods. In: DAGA 2008; 2008. .
3. de Klerk; Ossipov A. Operational Transfer Path Analysis: Theory, Guidelines and Tire Noise Application. Mechanical Systems And Signal Processing. 2010;24(7):1950–1962.
4. Cornelis D Petersen ACZCHH Ben S Cazzolato. Active Noise Control at a Moving Location Using Virtual Sensing. In: ICSV13-Vienna; 2006. .
5. GarciaBonito SBC J; Elliott. Generation of Zones of Quiet Using a Virtual Microphone Arrangement. Journal of The Acoustical Society of America. 1997;101(6):3498–3516.
6. Ipsen ICF. Numerical Matrix Analysis: Linear Systems and Least Squares. Society for Industrial and Applied Mathematics; 2009.
7. Jakob Putner AK Martin Lohrmann. Operational Transfer Path Analysis Predicting Contributions to The Vehicle Interior Noise for Different Excitations from the Same Sound Source. In: Proceedings of the Internoise 2012; 2012. .
8. A N Tikhonov VVSAGY A Goncharsky. Numerical Methods for the Solution of Ill-Posed Problems. Springer; 1995.